

ESTIMATION OF DYNAMIC PROPERTIES OF QUATERNARY ALLUVIAL SAND USING CYCLIC TRIAXIAL AND BENDER ELEMENT TESTS

Abhik Paul

Research Scholar, Dept. of Civil and Environmental Engineering
Indian Institute of Technology Patna, Patna-801106, India, Email id: abhik_1921ce04@iitp.ac.in

Pradipta Chakraborty*

Assistant Professor, Dept. of Civil and Environmental Engineering
Indian Institute of Technology Patna, Patna-801106, India, Email id: pradipt@iitp.ac.in

ABSTRACT

The Indo-Gangetic Quaternary alluvium predominantly consists of clay, silt, or sand layers as deposited by these major rivers and their tributaries. Sometimes, silts are intruded into the sand matrix, or plastic clay percolates into the sand matrix. The percolated plastic clay formed the alluvial lumps in the sand matrix at *in-situ* conditions due to groundwater fluctuations. From preliminary studies, it has been observed that these conditions affect the dynamic behaviour of these soils. However, the dynamic properties of these soils are not well documented. Therefore, a comprehensive study has been initiated here to estimate the dynamic behaviour of these various types of soil available in this Indo-Gangetic quaternary alluvial deposit. A series of large-strain cyclic triaxial tests and small-strain bender element tests were performed in the soil dynamics laboratory at IIT Patna. Samples were prepared by adding varying percentages (5%, 10%, 20%, and 30%) of non-plastic silt with sand, and mixing various percentages of clayey lumps with sand to evaluate the effect of these soil conditions. This methodology was used to examine the impact of silt and clay intrusion in the sand matrix on the liquefaction susceptibility of the soil. Findings indicate that lumped sandy soil demonstrates a higher susceptibility to liquefaction than clean sand. A novel aspect of this study is the comparison of dynamic shear modulus and damping ratios for clean sand and sand-lump mixtures, analysing the effects of saturation levels, silt content, and clayey lump percentages under cyclic loading. Simultaneously, bender element tests demonstrated that shear wave velocity increases with the increase in lump content, confining pressure, or loading frequency in the sand-lump mixture samples. The results contribute valuable insights into the behaviour of Gangetic alluvial soil under dynamic loading, enhancing geotechnical and seismic risk assessment in similar geological environments.

KEYWORDS: Shear Modulus, Damping Ratio, Lumps, Shear Wave Velocity, Cyclic Triaxial, Bender Element

INTRODUCTION

The Indo-Gangetic alluvial plain has been formed by the deposits of the Ganga, Indus, and Brahmaputra rivers and their tributaries. This Quaternary alluvium consists of predominantly clay, silt, or sand layers based on the locations and with respect to water velocity in these rivers. When the water velocity is higher, it can carry smaller particles and deposit larger particles. As the river reaches the plains, the water velocity becomes very slow and deposits these carried particles. Therefore, sand layers are dominant in the higher stretch of the river, whereas silt or clay layers are dominant in the lower stretch of these rivers. Due to river dynamics, alternate layers of sand and fine-grain soils are very frequent in these soil deposits. If the sand layer is overlaid by fine-grained soil, sometimes, silt or plastic clay particles can percolate into the sand matrix in these layered alluvial deposits. This intrusion of silts or clay in the sand matrix occurs during the rain. The percolated plastic clay formed alluvial lumps in the sand matrix at *in-situ* conditions due to groundwater fluctuations during and after rain (Das et al., 2020). These lumps can be challenging to separate during dry sieving because their sizes are comparable to those of coarse-grained soil (Paul and Chakraborty, 2024; Das et al., 2020). Such soil lumps are prevalent in alluvial deposits worldwide (Peterson et al., 2014). Additionally, the presence of these lumps in the sand matrix allows them to endure high vertical stress without significant volume changes; however, they are prone to a rapid and considerable reduction in volume upon exposure to water (Zamini and Badv, 2019). The assessment of the dynamic properties of this soil is important for the stability of structures on these soil deposits.

The Gangetic Plain can be broadly divided into three plains, namely Upper, Middle, and Lower Gangetic Plain (see Figure 1a). The past earthquakes in these plains have resulted in extensive casualties and structural damage, such as those observed in the 1833, 1934, and 1988 Bihar-Nepal, 2005 Kashmir, and 2015 Nepal earthquakes. This shows the critical need to understand the seismic behaviour of structures situated on these deposits. During these earthquakes, extensive soil liquefaction has been observed over a very large stretch. Liquefaction, a critical concern to geotechnical engineers, is a phenomenon where soil experiences a significant or complete reduction in shear strength and stiffness under cyclic or monotonic loading (Chakraborty et al., 2008; Popescu and Chakraborty, 2006). Past research has shown that seismic responses of soil are influenced by its dynamic properties, notably shear modulus and damping ratio, both of which impact the soil's behaviour under cyclic loading. These properties, alongside the soil's cyclic behaviour, are controlled by several factors, including loading frequency, loading amplitude, grain size distribution, confining pressure, global void ratio, intergranular void ratio, relative density, and degree of saturation (Kumar et al., 2018; Sitharam et al., 2004; Qian et al., 1991). Typically, loose, saturated, cohesionless soils are highly prone to liquefaction (Kumar et al., 2017; Kokusho, 1980). However, the behaviour of soil mixture with fine materials included within sand remains complex, particularly under seismic conditions. Various laboratory-based methods, such as bender element, resonant column, cyclic triaxial, and cyclic simple shear tests, have been used to estimate dynamic properties across different strain levels, revealing notable variability in soil behaviour with strain intensity (Hussain and Sachan, 2019; Kumar et al., 2018; Dutta et al., 2017; Gabrys et al., 2017). Based on degrees of saturation, soils are typically classified as dry, partially saturated, or fully saturated. While liquefaction is primarily a large-strain phenomenon in saturated sand, few studies have addressed how the different percentages of saturation affect soil behaviour under such conditions (Chakraborty et al., 2020; Tsukamoto et al., 2014). Those changes in the degree of saturation (Chakraborty et al., 2020; Jafarzadeh and Sadeghi, 2012) or the presence of gas in the soil skeleton (Lv and Zhang et al., 2022) can affect the dynamic properties and behaviour of the soil. In the past few years, the influence of silt intrusion in sand matrix on the development of excess pore water pressure has been studied extensively (Chakraborty et al., 2021; Nilay and Chakraborty, 2018; Karim and Alam, 2017; Dash and Sitharam, 2009; Polito and Martin, 2001; Thevanayagam et al., 2000). However, the influence of silt intrusion on the dynamic behaviour of sand in the Quaternary alluvial soil of the Indo-Gangetic plain has not been extensively studied.

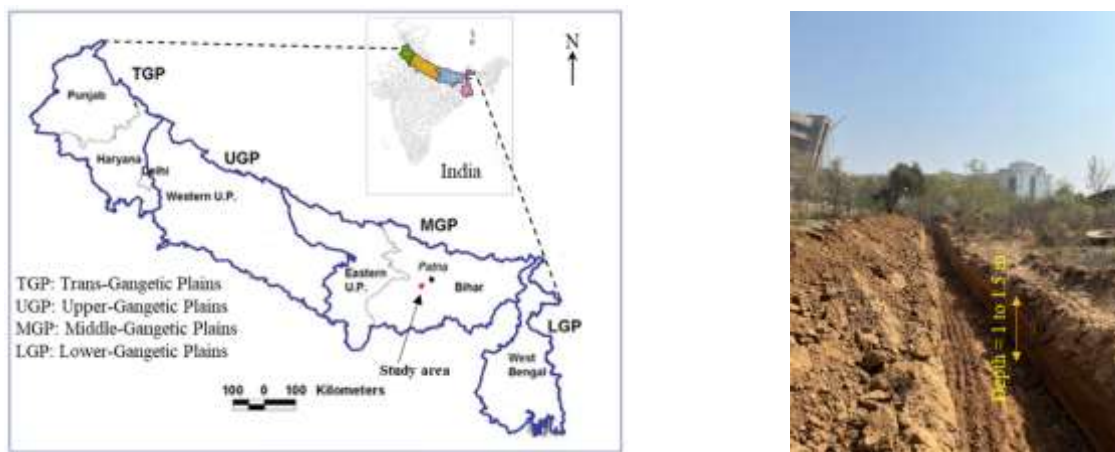


Fig. 1 (a) Site map showing Indo-Gangetic Plain; and (b) The transition layer from where the clayey lumps have been collected

Therefore, the present study has been initiated to address the influence of non-plastic silt and plastic clay lumps on the dynamic properties of the mixture. The present study is focused on the middle Ganga plain. The soil samples are collected from the Ganga and Sone basins at a depth of 1-3 m above and below the interface of fine- and coarse-grained soil layers (see Figure 1b). The reconstituted samples are prepared using the air pluviation technique documented in the literature. To estimate the dynamic properties of sand mixture for a wider range, triaxial and bender element samples are prepared for local Sone and Ganga sands mixed with varying silt and lump percentages (0%, 5%, 10%, 20%, 30%, and 100%). A series of large-strain cyclic triaxial tests and small-strain bender element tests were conducted in the soil dynamics laboratory at IIT Patna. A novel aspect of this study is the comparison of dynamic shear modulus and damping ratios for clean sand, sand intruded with various percentages of silts and clay lumps. Bender element tests demonstrated that shear wave

velocity (V_s) decreases with the increase in lump content and increases with the increase in confining pressure. The results indicated that soil lump intrusion in the sand matrix significantly influences the dynamic properties.

MATERIAL CHARACTERIZATION

The Indo-Gangetic Plain (IGP) represents one of India’s most agriculturally productive regions, accounting for approximately 15% of the country’s land area. Over time, the Ganga and its tributaries have deposited layers of gray-yellowish clay, silt, and sand across the floodplains in the Middle Ganga Plain (MGP). This natural soil on MGP consists of various percentages of silt mixed with sand or sometimes, lumps mixed with sand. The soil used in this study is locally obtained sand from the alluvial deposits of the Middle Ganga Plain, where the sand layers are primarily influenced by sedimentation from the Sone and Ganga rivers. Seasonal groundwater fluctuations, particularly during heavy rainfall or flooding, have shaped the structure of these water-transported soils. Groundwater levels typically rise during the monsoon (July-August) and decrease in the pre-monsoon period (April-May) as documented for this region by Saha and Sahu (2016). This cyclical rise and fall of groundwater levels leads to the formation of soil lumps, created when finer soil particles fill the voids among larger sand grains just above the groundwater table. These soil deposits have been documented in the Middle Ganga Plain, a subdivision of the IGB, by Paul and Chakraborty (2024) and Das et al. (2021). For this study, soil lumps were extracted from the interface between cohesive and cohesionless soil-dominant layers in the MGP, approximately 1.5 meters below the ground. At the time of collection, the groundwater depth was recorded at 8 meters, resulting in dry to partially saturated soil conditions. Observations indicate that natural soil in this area contains around 10-15% soil lumps by weight, though this percentage may vary by location. Additionally, silt for the study was obtained from the topsoil layer at the IIT Patna campus site, which is situated in MGP. The sand from the Sone and Ganga basins was also collected to identify the dynamic properties of various types of sand available in the region. As illustrated in Figure 2, Sone and Ganga River sands are classified as poorly graded sands, while clay lumps display low plasticity clay behaviour in wet sieving and poorly graded sand characteristics in dry sieving. The silt particles utilised in this study had a minimum particle size of approximately 45 micrometers. Table 1 documents key particle size distribution characteristics along with specific gravities for all samples, which range from 2.31 to 2.72. Maximum and minimum void ratios for the samples were estimated using vibratory table equipment as specified in IS-2720, Part-15.

Table 1: Properties of the Sone sand, Ganga sand, and clay lumps used in the study

Grain size range	Sone sand		Ganga sand	Silt	Lump	
	Natural	Medium grain			Wet sieving	Dry sieving
D ₅₀	0.304	0.584	0.201	0.021	0.019	1.402
D ₆₀	0.312	0.680	0.046	0.046	0.025	1.522
C _u	1.44	1.53	1.47	-	19.565	2.174
C _c	0.88	0.87	0.98	-	4.967	1.245
Coarse particles (%)	100	100	100	0	7.38	98.52
Fines (%)	0	0	0	100	92.62	1.48
Classification	Poorly graded	Poorly graded	Poorly graded	Non - Plastic	Low plasticity clay	Poorly graded sand
Specific gravity	2.65		2.67	2.72	2.31	

Table 2: All details of experiments performed for the present study

Sl. No.	Type of laboratory tests	Test name	Sample	Reference
1	Basic characterization tests	Sieve analysis, Hydrometer, Specific gravity	All sample	IS 2720, Part 4 IS 2720, Part 3
2	Dynamic properties measurement (Shear modulus, and damping ratio)	Strain-controlled cyclic triaxial tests	Sone sand: 100SS, 90SS10Si, 80SS20Si Ganga sand: 100GS, 90GS10Si, 80GS20Si Medium Sone sand: 100S, 90S10L, 80S20L	ASTM D-3999, 2003
3	Shear wave measurement (V_s)	Bender element tests	Medium Sone sand: 100S, 90S10L, 80S20L	ASTM D8295-19

Note: Si - Silt, S – Sand, GS – Ganga sand, SS – Sone sand and L – Lump

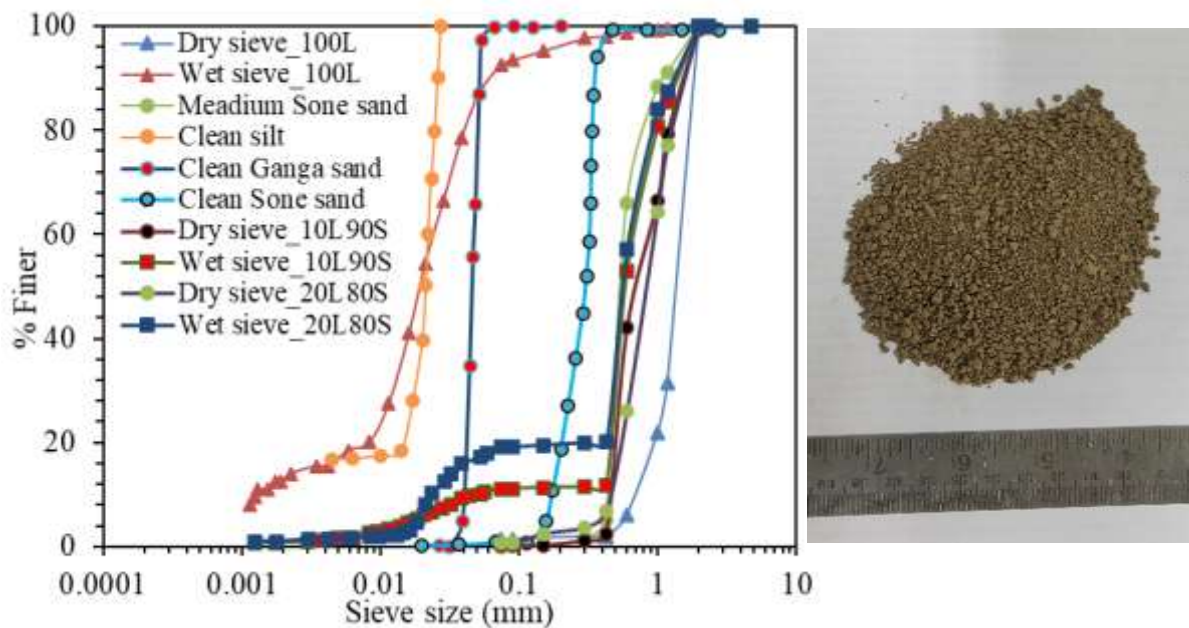


Fig. 2 (a) Grain size distribution curve, (b) Clayey lumps collected from the Middle Ganga plain (Note: L: Clay lumps; S: Sand)

SMALL-SCALE PHYSICAL EXPERIMENTS

This study investigates the dynamic properties of Sone and Ganga sands mixed with varying weights of non-plastic silt using strain-controlled cyclic triaxial tests. Additionally, the dynamic properties of sand-lump mixtures were examined through the same strain-controlled cyclic triaxial testing approach. The small-strain dynamic properties were estimated for the sand-lump mixture using bender element tests. All testing was carried out at the soil dynamics laboratory of IIT Patna, utilizing hydraulic-controlled cyclic triaxial equipment (see Figure 3) and bender element apparatus (see Figure 4). Details of these experiments are provided in Table 2. The cyclic triaxial tests were performed under undrained conditions on isotropically consolidated samples, while bender element tests were conducted on both dry and fully saturated conditions, following the standards outlined in ASTM D-5311 and ASTM D-8295-19. The testing details are briefed in the following sub-sections.

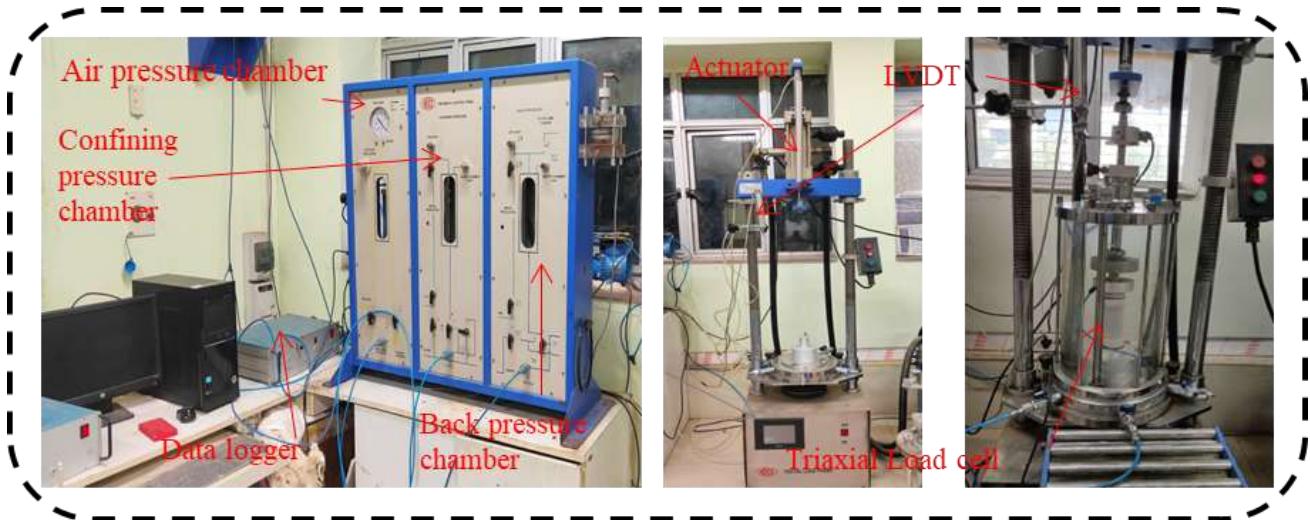


Fig. 3 Cyclic triaxial setup

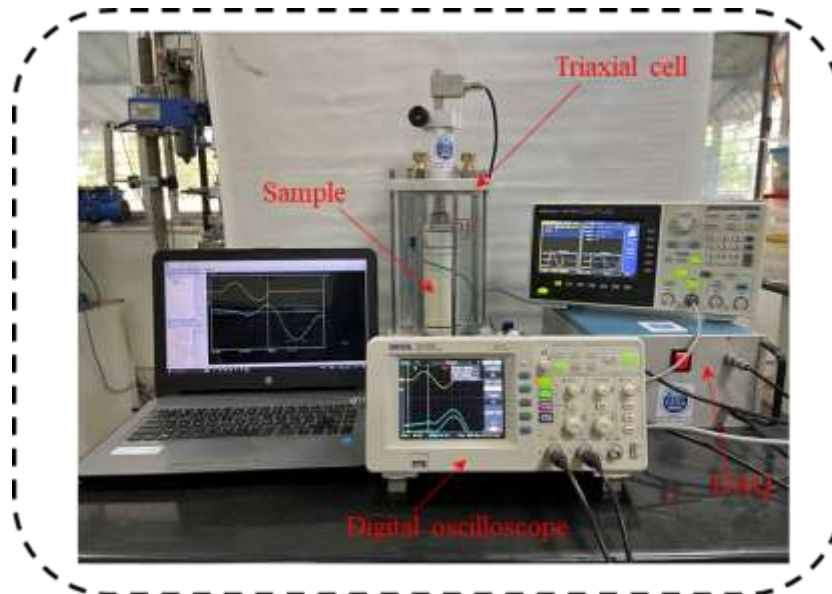


Fig. 4 Bender element test apparatus

1. Cyclic Triaxial Test

A series of strain-controlled cyclic triaxial tests was performed using a hydraulic-controlled apparatus, following ASTM D-5311-11 guidelines. Proper sample preparation is essential, as the changes in soil structure during preparation and saturation significantly affect the mechanical behaviour of cohesionless soils (Arthur and Menzies, 1972; Nemat-Nasser and Tobita, 1982). In this study, triaxial specimens were prepared in a split mould (38 mm in diameter and 76 mm in height) secured with a removable clamp. A vacuum was applied while placing the membrane to avoid necking during sample setup (Wijewickreme and Sanin, 2006). Samples were prepared using the dry pluviation method (see Figure 5) with a fixed diffuser, which allowed soil particles to fall freely from a predetermined height, achieving the target density (Dave and Dasaka, 2012; Raghunandan et al., 2012). To ensure an even distribution of particles along the mould circumference, horizontal shaking of the pluviator was applied during preparation, as recommended by Presti et al. (1993). Sample density was calculated based on the weight of soil added and the sample's volume, while a specific relationship between fall height and relative density was pre-established for fine- and medium-grained sands. Samples were prepared with almost similar low relative densities ($RD \leq 20\%$). The silty sand sample has been prepared at a constant relative density of the soil sample. With the addition of more and more silt in the initially sand-dominated matrix, it becomes a silt-dominated matrix. The limiting fine content (LFC) for the studied soil was estimated and reported by Chakraborty et al. (2021). After the dry pluviation, the sample was subjected to a suction of 10 kPa and

occasionally flushed with carbon dioxide gas to remove air from voids. De-air water was then introduced through the back-pressure line to achieve target saturation, confirmed by reaching the required Skempton's B parameter. After saturation, specimens were isotropically consolidated under an effective confining pressure of 150 kPa for silt-sand mixtures and 300 kPa for lump-sand mixtures. During strain-controlled testing, sinusoidal axial displacement was applied, with an axial deformation of ± 0.50 mm (axial strain, $\epsilon = 0.65\%$) and frequency of 1 Hz for silt-sand mixtures and an axial deformation of ± 0.15 mm and frequency of 1 Hz for lump-sand mixtures to replicate large strain cyclic loading conditions.

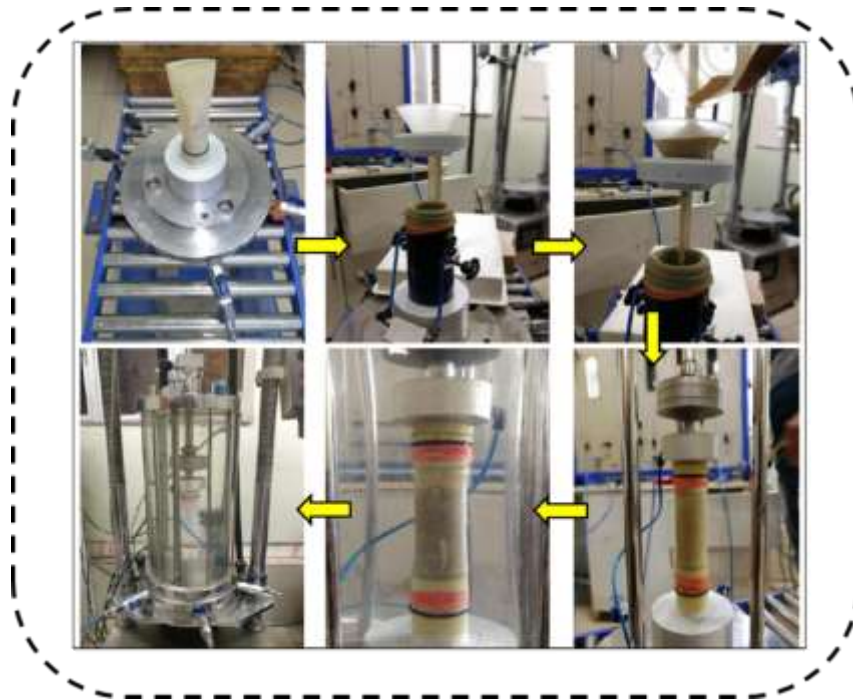


Fig. 5 Height and fall method to prepare samples for cyclic triaxial and bender element test using dry pluviation techniques

2. Bender Element Test

A series of bender element tests was conducted to measure the small-strain shear wave velocity (V_s) and estimate the corresponding shear modulus (G_0) of soil samples in the soil dynamics laboratory at IIT Patna. The bender element test setup consisted of a pair of bender elements, a transmitter, and a receiver, embedded at the top and bottom of the specimen within a cylindrical triaxial cell. The bender elements were horizontally oriented in this study to propagate shear waves in the direction perpendicular to the sample's longitudinal axis. A signal generator is used to generate waves. Both elements were connected to the oscilloscope for display and recording of generated and received signals. Soil samples were prepared with the dry pluviation method discussed in the previous section, and maintained the target relative density. In this study, specimens were prepared in a split mould of 50 mm in diameter and 100 mm in height. All the tests have been conducted in dry and fully saturated conditions. The test involved applying a sinusoidal wave pulse to the transmitting bender element at a frequency range of 1-10 kHz and a confining pressure range of 100-200 kPa. The wave generated by the transmitter travelled through the soil medium and was captured by the receiving element. The time delay between the transmitted and received wave was measured, representing the travel time of the shear wave across the sample length. Multiple tests were conducted to confirm the consistency of wave arrival time, and adjustments were made for any signal attenuation or noise interference. The testing procedure followed in this study to calculate shear wave velocity included both the "start-to-start" and "peak-to-peak" methods. In the "start-to-start" approach, V_s was calculated based on the initial rise of the wave signal from the transmitting element and the corresponding initial response in the receiving element. This method minimizes time delay inaccuracies associated with wave propagation. In the "peak-to-peak" method, the calculation used the time between the first major peak in the transmitted and received signals, allowing for comparison and validation of wave travel times. Both approaches provided insights into the wave transmission behaviour through the sample and were applied to ensure the accuracy of the V_s measurement. The V_s was then calculated using the following equation:

$$V_s = L/t \quad (1)$$

where L represents the sample height (distance between the bender elements), and t is the travel time of the wave. The value of V_s reflects the soil's small-strain stiffness, critical for evaluating its dynamic behaviour under seismic and cyclic conditions. Once V_s was determined, the small-strain G_0 could be calculated using the following equation:

$$G_0 = \rho V_s^2 \tag{2}$$

where ρ is the density of the soil sample. The G_0 reflects the soil's stiffness and resistance to shear deformation at small strains, which is critical for understanding its dynamic behaviour. Thus, the bender element test provides valuable insights into the mechanical properties of soil, aiding in the assessment of soil performance during seismic events.

LARGE STRAIN DYNAMIC SHEAR MODULUS

1. Effect of Silt Intrusion: Ganga and Sone Sand

The shear modulus is determined from strain-controlled cyclic triaxial tests. A Poisson's ratio of 0.4 has been assumed for cohesionless soils, as suggested by Ghayoomi et al. (2017). Young's modulus (E) values were calculated separately under both extension and compression loading, with the average of these values used to compute the shear modulus using the following equation:

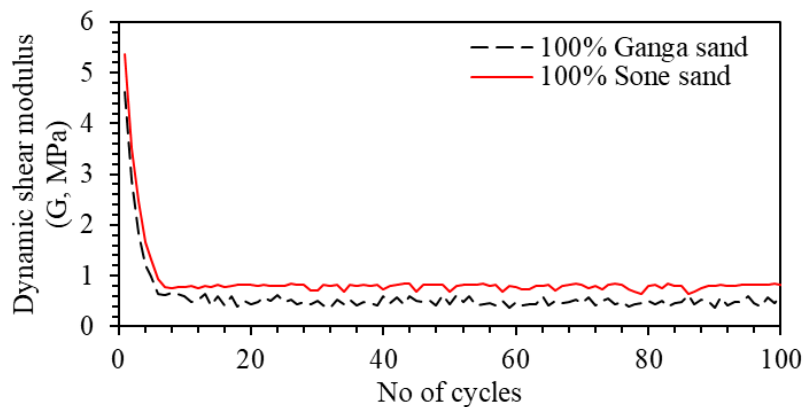


Fig. 6 Effect of soil gradation on dynamic shear modulus for 100% Ganga sand

$$G = \frac{E}{2 \times (1 + \mu)} \tag{3}$$

where E is Young's modulus and μ is the Poisson ratio. As discussed in the earlier section, soil deposit MGP is influenced by the deposition of the river Ganges and its tributaries. Therefore, to estimate the effect of soil fabric, the dynamic shear modulus for clean Ganga and Sone River sand has been estimated and shown in Figure 6. In comparing the shear modulus (G) of clean Ganga and Sone sands (see Figure 6), it is observed that Ganga sand consistently exhibits a lower G value than Sone sand, indicating that Sone sand possesses higher strength. This can be directly linked with the rock of the source location through which these rivers travel. The Sone River originated from Pendra in Amarkantak Hill and travelled through the Kaimur Range before merging with the Ganga near Maner. The rock in this area comprises mostly Basalt rock of the Deccan Traps, which is stronger in nature. Whereas Ganga originates from Gangotri and travels through various rocky areas comprised of Sedimentary and metamorphic rock. So, the sand in the Sone River originated from these harder basalt rocks poses higher strength. The G of clean sand was initially observed to be relatively high, with values around 4.5 to 5.4 MPa under low cyclic strain (e.g., at initial cycles) for the clean Ganga and Sone sand, respectively. As cyclic loading increases, the G decreases gradually due to the development of excess pore water pressure (presented by Chakraborty et al., 2021). At higher strain levels, the modulus of clean sand reduced to around 0.45 and 0.85 MPa for the same sample, indicating a loss of stiffness under repeated loading cycles.

Figure 7 illustrates the variations in G values due to the intrusion of silt in the sand matrix for Ganga and Sone sands. The results demonstrate that the Sone sand-silt mixtures degrade slowly compared to the Ganga sand-silt mixtures. This higher dynamic shear modulus indicates that the soil is stiffer and less prone to deformation under cyclic loads. In contrast, both sands mixed with 10 to 20% non-plastic fines exhibited a slightly higher initial dynamic shear modulus (see Figure 7). When 30% silt is mixed with Sone sand (70SS30Si) the initial shear modulus decreases to 5.14 MPa. The same behaviour was also observed for 30% silt mixed with

Ganga sand. The value of G has been observed as 3.45 MPa for this sample (70GS30Si). However, the Ganga sand-silt mixture showed a higher reduction in modulus with increasing cyclic load. This important behaviour of the sand-silt mixture can be explained using LFC discussed earlier and in Chakraborty et al. 2021. This comparison highlights how the presence of silt in the sand matrix influences the dynamic stiffness of the soil.

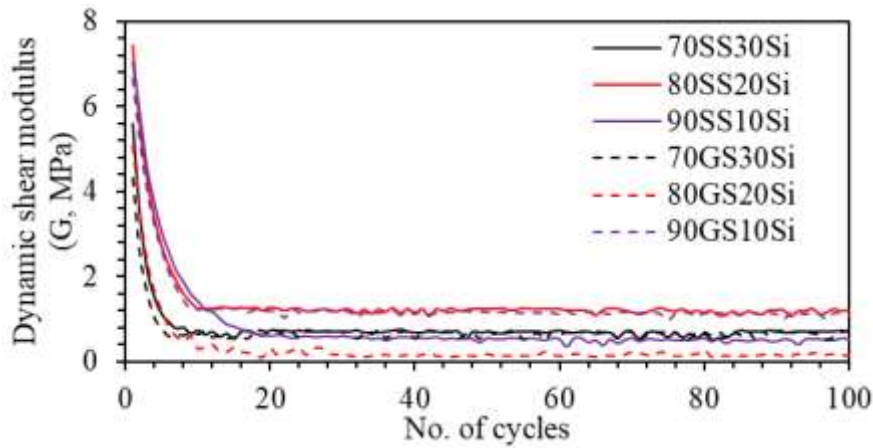


Fig. 7 Effect of Silt content on dynamic shear modulus (Note: SS- Sone sand; GS- Ganga Sand; Si- Silt)

2. Effect of Lumps Intrusion: Medium Sone Sand

The presence of lumps in a sand matrix was found to significantly influence the dynamic shear modulus (G) of natural Sone sand (Das et al., 2021). In this study, the G for the medium-grain Sone sand has been estimated from cyclic triaxial tests. Three distinct medium sand-lump mixtures were tested under cyclic loading: 90% sand with 10% lumps, 80% sand with 20% lumps, and 70% sand with 30% lump content (see Figure 8). The results indicate a clear decreasing trend for dynamic shear modulus with increasing lump content. For the mixture with 90% sand and 10% lump content, the initial dynamic shear modulus decreased from 15.8 MPa to 0.65 MPa within 95 cycles of loading. Similarly, the mixture containing 80% sand and 20% lump content showed a reduction in modulus from 12.31 MPa to 3.07 MPa within 95 cycles of loading. In the mixture with 70% sand and 30% lump content, the shear modulus dropped from 11.4 MPa to 1.1 MPa within 95 cycles of loading. All the decreasing shear moduli have been presented in Figure 8 for the first 150 cycles. This reduction in G across all mixtures suggests that increasing the lump content in sand contributes to a gradual reduction in the soil's initial dynamic stiffness and cyclic strength (as reported by Chakraborty et al., 2021). The reduction in dynamic shear modulus can be attributed to the increasing void ratio that accompanies higher lump percentages. As the lump content increases, voids within the soil matrix also increase, creating pathways for air to enter at saturation levels above 95%. The entrapped air, which is much more compressible than water, absorbs a significant portion of the applied cyclic stresses. As a result, these stresses are initially taken up by the air-laden pore water, delaying their transfer to the soil skeleton. This process leads to a softer response under cyclic loads, thereby reducing the specimen's dynamic shear modulus. This observation underscores the weakening effect of lump content on the soil's resistance to cyclic loading, due to both the structural alterations within the soil matrix and the impact of air-filled voids. Consequently, higher lump percentages in the sand may compromise the soil's performance in applications where cyclic stability and stiffness are crucial.

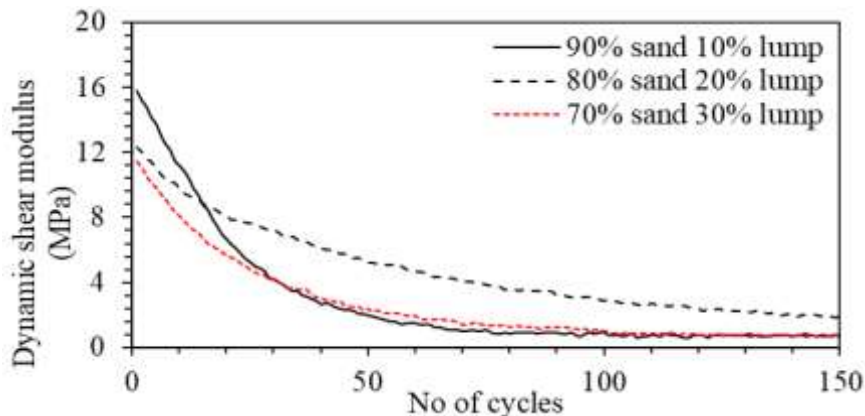


Fig. 8 Effect of clayey lump intrusion in the medium sand matrix on dynamic shear modulus

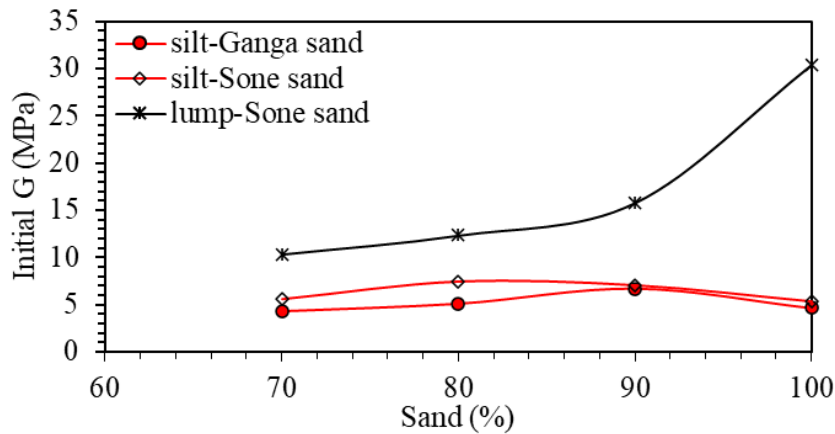


Fig. 9 Variation of initial dynamic shear modulus with increasing silt or lump percentages

The initial dynamic shear moduli of all the samples have been compared and shown in Figure 9. Those initial G values showed a distinct trend across different sand mixtures, reflecting the effect of both lump and silt inclusions on sand's stiffness. For the medium Sone sand intruded with soil lumps, the initial G values progressively decrease with increasing lump content. For example, the initial G value decreased from 30.33 MPa for the 0% lump content to 10.32 MPa at 70% lump content in the lump-sand mixture. This reduction suggests that higher lump content introduces structural heterogeneity and larger void spaces within the matrix, which weakens the sand's resistance to shear deformations under cyclic loading conditions. The increased void ratio allows for more deformation, as documented by prior studies, which have shown that the addition of softer, deformable inclusions in sand matrices often results in lower stiffness and higher compressibility (Ghayoomi et al., 2017). For the sand-silt mixtures, a somewhat different trend is observed. With Sone sand, the highest initial G values are recorded at intermediate silt contents, reaching 7.42 MPa for the sand intruded with 20% silt, compared to 5.598 MPa for 30% silt and 7.04 MPa for 10% silt. Interestingly, the pure Sone sand sample shows a lower initial G value of 5.35 MPa, indicating that a moderate amount of non-plastic fines may initially contribute to denser packing and higher stiffness, but excessive silt content could lead to an overall decrease in modulus due to inter-particle slippage or reduced contact points. Similar findings were observed in the Ganga sand-silt mixtures, where the initial G values were highest at 6.65 MPa for 90% sand intruded with 10% silt, but decreased to 4.309 MPa with 30% silt, as well as 4.62 MPa for pure Ganga sand. This trend aligns with previous observations that non-plastic fines can initially increase the modulus by enhancing particle packing density but will reduce stiffness when their proportion is too high, resulting in weaker structural integrity within the sand matrix (Presti et al., 2016). Overall, these findings underscore the physical significance of the dynamic shear modulus in assessing soil stiffness and the capacity of the soil matrix to transmit and resist cyclic shear stresses. Dynamic behaviour under cyclic loads is notably influenced by the matrix composition, with lump and silt content directly impacting the soil's ability to maintain its structure under dynamic stress, a critical factor for geotechnical applications in seismic-prone regions.

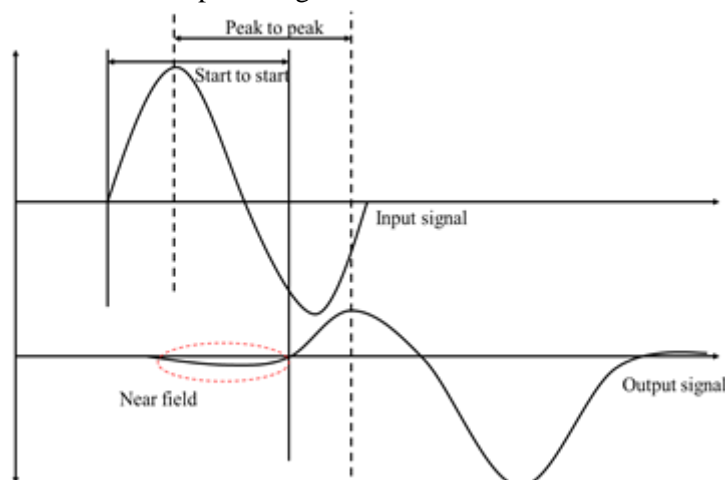


Fig. 10 Typical velocity calculation procedure by two different methods (S-S and P-P)

SMALL STRAIN DYNAMIC SHEAR MODULUS: EFFECT OF LUMPS INTRUSION

Determining travel time (Δt) in bender element (BE) tests has become increasingly common but remains challenging due to subjectivity and inherent uncertainties, primarily arising from near-field effects and signal distortions. Various interpretation methods, such as start-to-start (S-S), peak-to-peak (P-P), cross-correlation (CC), and cross-power (CP) techniques, have been suggested in the literature to estimate travel time, each offering unique approaches and insights (Viana da Fonseca et al., 2009; Lee and Santamarina, 2005). However, these methods can produce varied results, and no consensus has been reached regarding the most accurate or reliable approach. For the current study, both the S-S and P-P methods are applied to calculate V_s , in order to assess their effectiveness and reliability. Figure 10 shows the input and output signals for calculating the V_s . Different frequencies and confining pressure can affect the receiving signal. Firstly, the specimen was prepared at a low relative density (less than 15%). Different confining pressures (100 kPa, 200 kPa) and different frequencies have been used to estimate the V_s . The V_s of clean, medium Sone sand were evaluated using both the S-S and P-P methods across a range of frequencies (1, 5, 10, and 15 kHz) under confining pressures of 100 kPa and 200 kPa (Figure 11). The S-S method at 100 kPa showed an increase in V_s from 204 m/s at 1 kHz to 273 m/s at 15 kHz, while the P-P method yielded slightly higher velocities, peaking at 261 m/s at 15 kHz. A similar trend was observed at 200 kPa, where V_s increased from 204 m/s at 1 kHz to 316 m/s at 15 kHz using the S-S method, and from 226 m/s to 304 m/s with the P-P method (Figure 11).

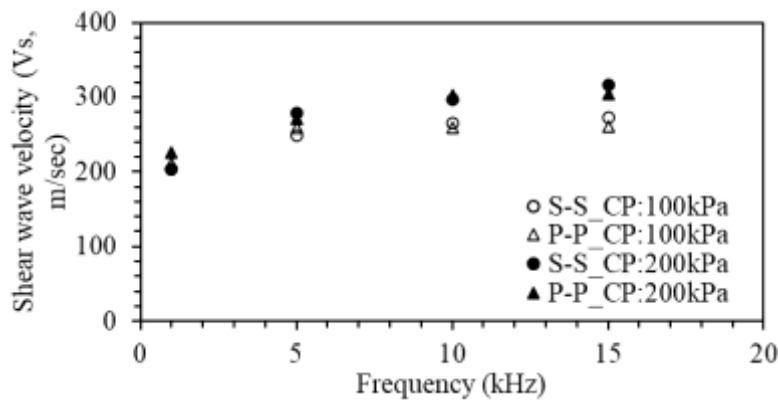


Fig. 11 Change in shear wave velocities with increasing frequencies at different confining pressures for clean medium sand

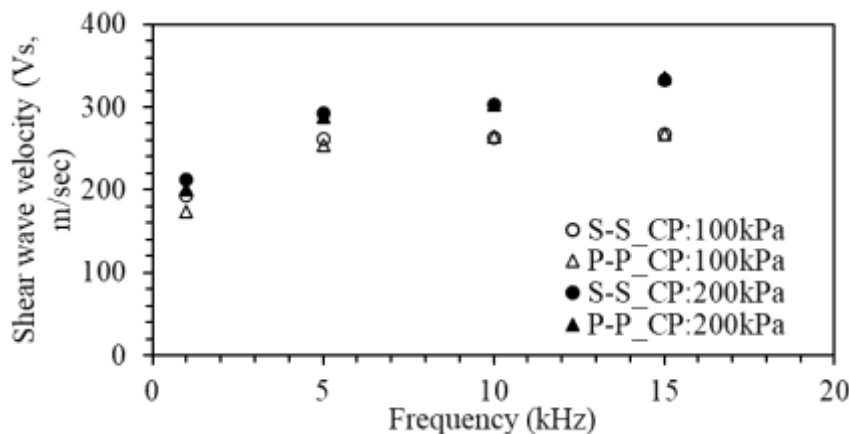


Fig. 12 Change in shear wave velocities with increasing frequencies for medium-grained Sone sand intruded with 20% lumps

For the medium-grained Sone sand intruded with 20% lumps, V_s was derived using both the S-S and P-P methods for the same different input frequencies and confining pressures as shown in Figure 12. This percentage was selected for comparison as the maximum clay lumps content in the natural deposit by the Sone River has been found as 18-20%, as mentioned in the earlier section. At 100 kPa, the velocities derived from the S-S method range from 193 to 267 m/s, while those obtained from the P-P method range from 174 to 268 m/s. At the higher confining pressure of 200 kPa, the V_s values are slightly higher, increased from 212 to 333 m/s using

the S-S method and from 200 to 336 m/s using the P-P method. These trends illustrate an increase in V_s with both frequency and confining pressure. This has been aligned with the established behaviour in soil dynamics, where higher confining pressure typically results in a stiffer soil matrix and thus higher shear wave velocities. When compared to clean medium Sone sand, the mixture containing 20% lumps generally exhibits a slightly lower V_s , particularly at the lower frequencies. This can be attributed to the lumps acting as void fillers, which alter the soil's packing density and potentially introduce more compressible zones within the matrix. Prior studies have shown that the presence of different particle sizes, especially the inclusion of less rigid lumps, can reduce soil stiffness and lead to more complex wave propagation characteristics under cyclic loading (Ghayoomi et al., 2017). These results also reveal that V_s increases with both confining pressure and frequency. Higher confining pressures typically reduce void ratios, thus stiffening the soil structure, which leads to higher shear wave velocities. This finding aligns with previous studies indicating that denser soil matrices or increased effective stresses often produce higher V_s values due to a more rigid particle arrangement (Santamarina et al., 2001). The observed frequency-dependent increase in V_s may relate to the dispersion effects in sandy soils, where higher frequencies can increase wave speed due to reduced particle lag and interference, as noted in studies by Viggiani and Atkinson (1995).

For the clean medium Sone sand, the small-strain shear modulus (G) was evaluated from bender element tests and shown in Figure 13. The results revealed that at a confining pressure of 100 kPa, G increased with frequency, reaching 29.93 MPa at 15 kHz using the S-S method and 26.737 MPa using the P-P method. Similarly, at a confining pressure of 200 kPa, G showed a notable increase in frequency, achieving a maximum of 40.109 MPa at 15 kHz with the S-S method and 37.121 MPa with the P-P method. Physically, these results suggest that the dynamic shear modulus, which directly depends on V_s will decrease as lump content increases, even as confining pressure provides some compensation. Notably, this study highlights the role of lump content in modifying soil stiffness, especially in sands intended for foundation applications. Further investigation could examine how lump distribution within the matrix influences the formation of rigid soil skeletons, as well as the impact on soil behaviour under seismic loading conditions. The differences between the S-S and P-P methods highlight the influence of interpretation techniques on V_s values. This variation is common in bender element tests, where S-S is often used for more conservative values and P-P for potentially higher estimates. The discrepancies suggest that while both methods can be reliable, the choice depends on the desired application and required accuracy (Viana da Fonseca et al., 2009). The results suggest that increasing frequency at elevated pressures could provide more consistent V_s measurements, potentially reducing the influence of method-induced variation.

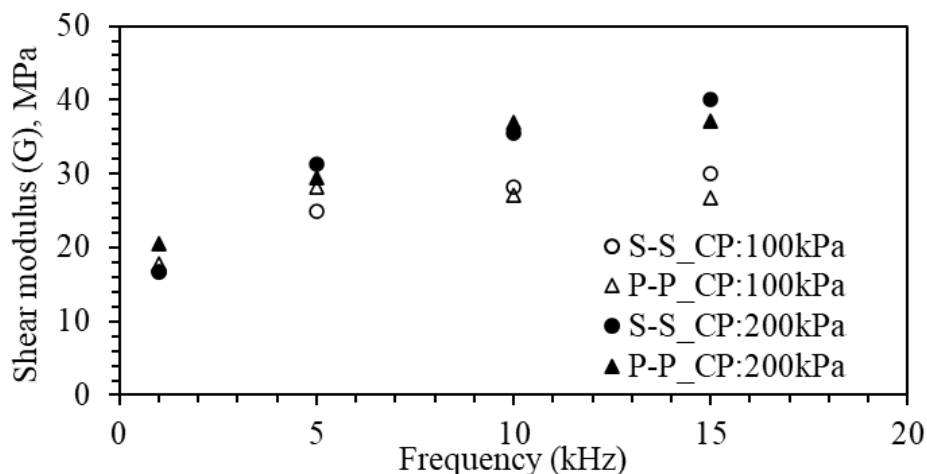


Fig. 13 Change in small strain shear modulus with increasing frequencies at different confining pressures for clean medium sand

LARGE STRAIN DAMPING RATIO

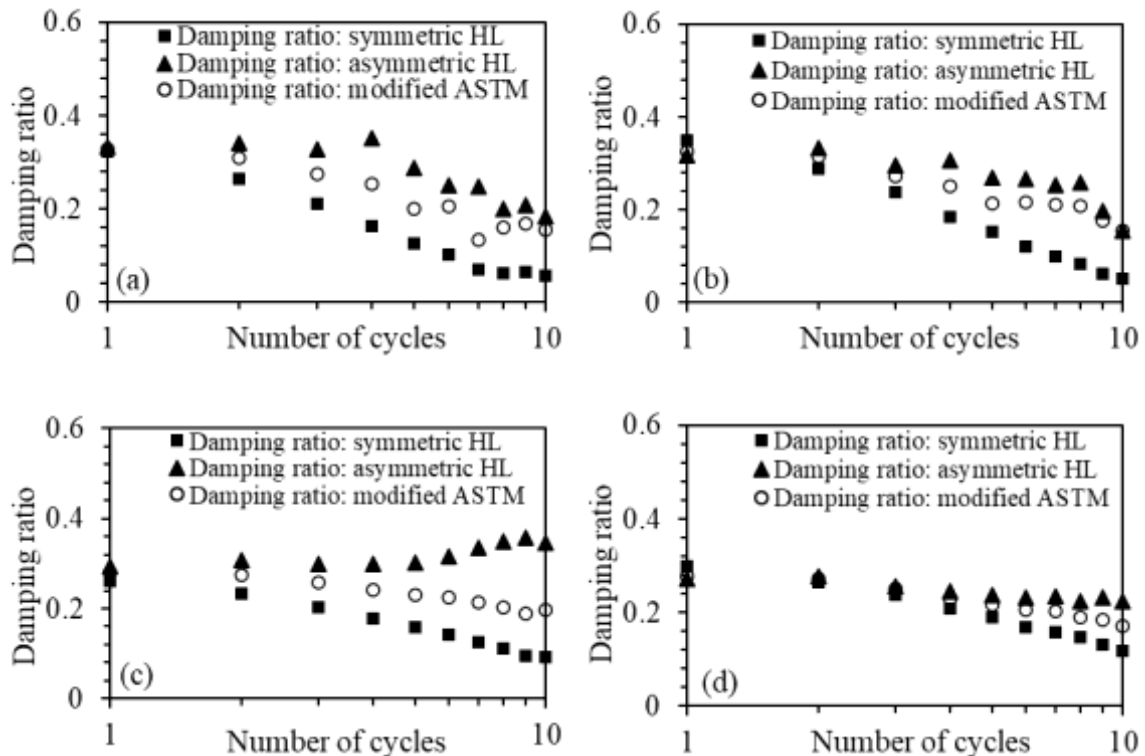
1. Effect of Silt Intrusion: Ganga and Sone Sand

The damping ratio is another essential dynamic property that characterizes the cyclic response of soils under dynamic loading. While the shear modulus is unaffected by the symmetry of the hysteresis loop, the damping ratio directly relates to the loop shape, as it represents the energy dissipation within the soil matrix (Kumar et

al., 2017; Kokusho, 1980). This study employs three distinct methods for evaluating the damping ratio: (a) symmetric hysteresis loop (SHL) method, (b) asymmetric hysteresis loop (AHL) method, and (c) modified ASTM method, which adjusts for loop asymmetry typically observed in cyclic triaxial tests. The SHL method, based on ASTM D3999, assumes a symmetric loop shape, a standard approach in earlier studies (Kumar et al., 2017; ASTM D-3999). However, cyclic triaxial tests often produce loops that are not perfectly symmetric, possibly due to complex soil behaviour under cyclic stress (Jaya et al., 2012). Recognising this, the AHL and modified ASTM methods were developed to incorporate the observed asymmetry, offering a more accurate measure of damping ratio for non-symmetric loops and thus better representing actual energy dissipation under cyclic loading (Das and Chakraborty, 2022). Figure 14 compares the estimated damping ratios for clean Ganga and Sone sands, Ganga sand-silt, and Sone sand-silt mixtures. For Ganga and Sone sand-silt mixtures, the modified ASTM approach tends to produce lower damping ratios than the AHL method but higher than those from the SHL method. This pattern likely arises because both AHL and modified ASTM methods incorporate the asymmetry seen in cyclic triaxial testing, capturing the energy dissipation more accurately than the SHL method.

2. Effect of Lumps Intrusion: Medium Sone Sand

Figure 15 compares the damping ratios for lump-medium sand mixtures for two different silt proportions. The modified ASTM method produces damping ratios that are underestimated in SHL but overestimated in the AHL, suggesting that particle size distribution and coarser particles in lump-sand mixtures influence damping differently. Additionally, as the number of loading cycles increases, the damping ratio shows a downward trend, possibly due to structural rearrangements within the soil matrix. This rearrangement affects soil stiffness, subsequently impacting the damping characteristics. These findings underscore the need for method selection that aligns with soil composition and particle dynamics, as the energy dissipation behaviour in mixed soils can vary significantly under cyclic loading.



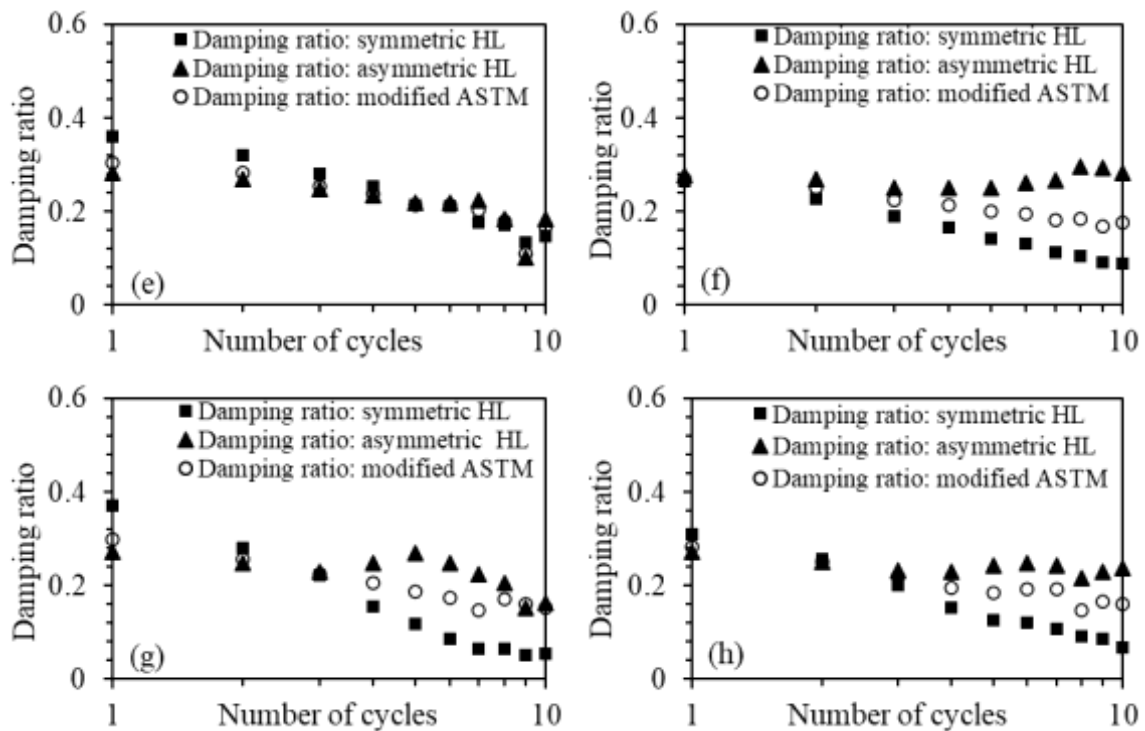


Fig. 14 Damping ratio as a function of number of loading cycles for various percentage of silt (a) 100% Ganga sand; (b) 100% Sone sand; (c) 90% Ganga sand 10% silt mixture (d) 90% Sone sand 10% silt mixture; (e) 80% Ganga sand 20% silt mixture; (f) 80% Sone sand 20% silt mixture (g) 70% Ganga sand 30% silt mixture; (h) 70% Sone sand 30% silt mixture (Note: HL is hysteresis loop)

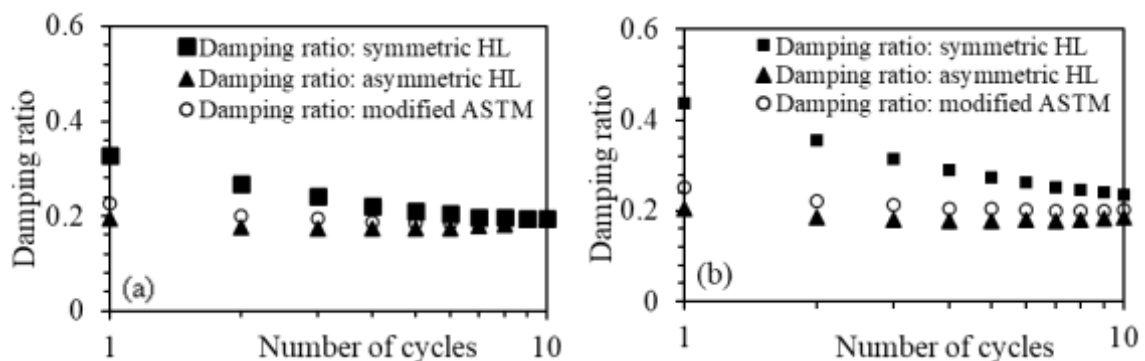


Fig. 15 Damping ratio as a function of the number of loading cycles for various percentages of lumps (a) 90% sand 10% lumps mixture (b) 80% sand 20% lumps mixture

CONCLUSIONS

This research paper assesses the dynamic properties of quaternary alluvial sand intruded with silt and lumps through a combination of cyclic triaxial and bender element tests. By employing various confining pressures and frequencies, this study provides a comprehensive estimation of the V_s , the small and large strain shear modulus of clean and clay lump intruded medium Sone sand, and silt intruded Ganga and Sone sands. The results highlight the influence of lump and silt content on the dynamic behaviour of the Ganga and Sone River sands. The following conclusions can be drawn from this study:

- The findings illustrate that the dynamic properties of quaternary alluvial sand significantly vary with confining pressure and frequency, demonstrating the critical role these parameters play in assessing soil behaviour under cyclic loading. Soils with higher dynamic shear modulus values can better support loads and resist excessive settlements or lateral displacements. A lower modulus under cyclic loading can indicate a higher risk of soil structure collapse, leading to liquefaction.

- The inclusion of silt in the sand matrix of Ganga and Sone sand leads to significant changes in dynamic shear modulus (G). The results indicate that as the silt content increases, the initial G value increases up to 80% for Sone sand and 90% for Ganga sand and decreases thereafter. The effect of lumps intrusion in the sand matrix is more visible as the initial G decreased continuously with the increase in lumps content. This reflects a decline in sand stiffness and strength due to the intrusion of silt or lumps under cyclic loading conditions.
- The results indicate a significant decrease in shear wave velocity (V_s) as the lump content increases in the sand-lump mixture. Specifically, the clean medium Sone sand demonstrated higher V_s values compared to mixtures containing 20% lump content. This shows that the presence of non-plastic inclusions can adversely affect the dynamic response of granular materials.
- The frequency and confining pressure have a notable impact on the measured shear wave velocities and shear modulus (G). As the frequency and confining pressure increase, both V_s and G show an upward trend. This observation emphasized the importance of confining pressure in dynamic soil behaviour. Higher confining pressure improved the stiffness and stability of the soil.

Those findings have significant implications for the design and analysis of soil structures, particularly in areas (Middle Ganga Plain) where sands are mixed with varying percentages of lump and silt materials. Understanding how these mixtures behave under dynamic loading conditions is essential for accurate predictions of soil performance in geotechnical applications, aiding in the development of more robust foundation and stability designs. These conclusions highlight the need for further research into the behaviour of silt-sand and lump-sand mixtures, particularly under varying environmental conditions and loading scenarios, to develop more effective design guidelines for geotechnical structures.

ACKNOWLEDGEMENT

The authors acknowledge the Department of Higher Education (Govt. of India) and the Indian Institute of Technology Patna for providing the funding to carry out the doctoral research of the first author, for which no specific grant number is allotted. The authors also acknowledge the Department of Atomic Energy, Board of Research in Nuclear Sciences, for providing funding (No: 51/14/04/2022-BRNS) for doing research in this area.

REFERENCE

1. Arthur, J.R.F. and Menzies, B. (1972). "Inherent Anisotropy in a Sand", *Geotechnique*, Vol. 22, No. 1, pp. 115-128. <https://doi.org/10.1680/geot.1972.22.1.115>
2. ASTM D 8259-19 (2019). "Standard Test Method for Determination of Shear Wave Velocity and Initial Shear Modulus in Soil Specimens Using Bender Elements", *ASTM International*.
3. ASTM D3999 (2011). "Standard Test Methods for the Determination of the Modulus and Damping Properties of Soils Using the Cyclic Triaxial Apparatus", *Annual Book of ASTM Standards, ASTM International, West Conshohocken, PA*.
4. ASTM D5311-92 (1996). "Standard Test Method for Load Controlled Cyclic Triaxial Strength of Soil", *ASTM International, West Conshohocken, PA*.
5. Chakraborty, P., Nilay, N. and Das, A. (2021). "Effect of Silt Content on Liquefaction Susceptibility of Fine Saturated River Bed Sands", *International Journal of Civil Engineering*, Vol. 19, pp. 549-561. <https://doi.org/10.1007/s40999-020-00574-9>
6. Chakraborty, P., Roshan, A.R. and Das, A. (2020). "Evaluation of Dynamic Properties of Partially Saturated Sands Using Cyclic Triaxial Tests", *Indian Geotechnical Journal*, Vol 50, No. 6, pp. 948-962. <https://doi.org/10.1007/s40098-020-00433-3>
7. Chakraborty, P., Popescu, R., Phillips, R. and Dief, H. (2008). "Liquefaction of Heterogeneous Soil: Centrifuge Study", *Proceedings of International Association for Computer Methods and Advances in Geomechanics*, pp. 1389-1396.
8. Das, A. and Chakraborty, P. (2022). "Simple Models for Predicting Cyclic Behaviour of Sand in Quaternary Alluvium", *Arabian Journal of Geosciences*, Vol. 15, No. 5, pp. 385. <https://doi.org/10.1007/s12517-022-09639-6>

9. Das, A., Chakraborty, P. and Popescu, R. (2021). "Assessment of Lumped Particles Effect on Dynamic Behaviour of Fine and Medium Grained Sands", *Bulletin of Earthquake Engineering*, Vol. 19, No. 2, pp. 745-766. <https://doi.org/10.1007/s10518-020-01012-w>
10. Das, A. and Chakraborty, P. (2020). "Influence of Motion Energy and Soil Characteristics on Seismic Ground Response of Layered Soil", *International Journal of Civil Engineering*, Vol. 18, No. 7, pp. 763-782. <https://doi.org/10.1007/s40999-020-00496-6>
11. Dash, H.K. and Sitharam. T.G. (2009). "Undrained Cyclic Pore Pressure Response of Sand-Silt Mixtures: Effect of Nonplastic Fines and Other Parameters", *Geotechnical and Geological Engineering*, Vol. 27, pp. 501-517. <https://doi.org/10.1007/s10706-009-9252-5>
12. Dave, T.N. and Dasaka, S.M. (2012). "Assessment of Portable Traveling Pluviator to Prepare Reconstituted Sand Specimens", *Geomechanics and Engineering*, Vol. 4, No. 2, pp. 79-90.
13. Dutta, T.T., Saride, S. and Jallu, M. (2017). "Effect of Saturation on Dynamic Properties of Compacted Clay in a Resonant Column Test", *Geomechanics and Geoengineering*, Vol. 12, No. 3, pp. 181-190. <https://doi.org/10.1080/17486025.2016.1208849>
14. Gabryś, K., Sas, W., Soból, E. and Głuchowski, A. (2017). "Application of Bender Elements Technique in Testing of Anthropogenic Soil-Recycled Concrete Aggregate and its Mixture with Rubber Chips", *Applied Sciences*, Vol. 7, No. 7, pp. 741. <https://doi.org/10.3390/app7070741>
15. Ghayoomi, M., Suprunenko, G. and Mirshekari, M. (2017). "Cyclic Triaxial Test to Measure Strain-Dependent Shear Modulus of Unsaturated Sand", *International Journal of Geomechanics*, Vol. 17, No. 9, pp. 04017043. [https://doi.org/10.1061/\(asce\)gm.1943-5622.00009](https://doi.org/10.1061/(asce)gm.1943-5622.00009)
16. Hussain, M. and Sachan, A. (2020). "Dynamic Behaviour of Kutch Soils Under Cyclic Triaxial and Cyclic Simple Shear Testing Conditions", *International Journal of Geotechnical Engineering*, Vol. 14, No. 8, pp. 902-918. <https://doi.org/10.1080/19386362.2019.1608715>
17. Jafarzadeh, F. and Sadeghi, H. (2012). "Experimental Study on Dynamic Properties of Sand with Emphasis on the Degree of Saturation", *Soil Dynamics and Earthquake Engineering*, Vol. 32, No. 1, pp. 26-41. <https://doi.org/10.1016/j.soildyn.2011.08.003>
18. Jaya, V., Dodagoudar, G.R. and Boominathan, A. (2012). "Modulus Reduction and Damping Curves for Sand of South-East Coast of India", *Journal of Earthquake and Tsunami*, Vol. 6, No. 04, pp. 1250016. <https://doi.org/10.1142/s1793431112500169>
19. Karim, M.E. and Alam, M.J. (2017). "Effect of Nonplastic Silt Content on Undrained Shear Strength of Sand-Silt Mixtures", *International Journal of Geo-Engineering*, Vol. 8, pp. 1-26. <https://doi.org/10.1186/s40703-017-0051-1>
20. Kokusho, T. (1980). "Cyclic Triaxial Test of Dynamic Soil Properties for Wide Strain Range", *Soils and Foundations*, No. 20, No. 2, pp. 45-60.
21. Kumar, S.S., Krishna, A.M. and Dey, A. (2018). "High Strain Dynamic Properties of Perfectly Dry and Saturated Cohesionless Soil", *Indian Geotechnical Journal*, Vol. 48, pp. 549-557. <https://doi.org/10.1007/s40098-017-0255-5>
22. Kumar, S.S., Krishna, A.M. and Dey, A. (2018). "Dynamic Properties and Liquefaction Behaviour of Cohesive Soil in Northeast India Under Staged Cyclic Loading", *Journal of Rock Mechanics and Geotechnical Engineering*, Vol. 10, No. 5, pp. 958-967. <https://doi.org/10.1016/j.jrmge.2018.04.004>
23. Kumar, S.S., Krishna, A.M. and Dey, A. (2017). "Evaluation of Dynamic Properties of Sandy Soil at High Cyclic Strains", *Soil Dynamics and Earthquake Engineering*, Vol. 99, pp. 157-167. <https://doi.org/10.1016/j.soildyn.2017.05.016>
24. Lee, J.S. and Santamarina, J.C. (2005). "Bender Elements: Performance and Signal Interpretation", *Journal of Geotechnical and Geoenvironmental Engineering*, Vol. 131, No. 9, pp. 1063-1070. [https://doi.org/10.1061/\(asce\)1090-0241\(2005\)131:9\(1063\)](https://doi.org/10.1061/(asce)1090-0241(2005)131:9(1063))
25. Lv, M. and Zhang, D. (2022). "Liquefaction Mitigation of Medium-To-Fine Sands with Microbial Gas Under Cyclic Triaxial Loading", *International Journal of Civil Engineering*, Vol. 20, No. 9, pp. 1085-1099. <https://doi.org/10.1007/s40999-022-00727-y>

26. Nemat-Nasser, S. and Tobita, Y. (1982). "Influence of Fabric on Liquefaction and Densification Potential of Cohesionless Sand", *Mechanics of Materials*, Vol. 1, No. 1, pp. 43-62. [https://doi.org/10.1016/0167-6636\(82\)90023-0](https://doi.org/10.1016/0167-6636(82)90023-0)
27. Nilay, N. and Chakraborty, P. (2018). "Evolution in Liquefaction Strength of Ganga River Sand Due to the Intrusion of Non-Plastic Silt", *In: Indian Geotechnical Conference, IGC 2018 IISC Bangaluru, December 13-15*.
28. Paul, A. and Chakraborty, P. (2024). "Microstructural Characterization of Alluvial Sand Containing Cohesive Soil Lumps During Loading and Inundating", *International Journal of Civil Engineering*, pp. 1-18. <https://doi.org/10.1007/s40999-024-00974-1>
29. Peterson, C.D., Grathoff, G.H., Reckendorf, F., Percy, D. and Price, D.M. (2014). "Late Pleistocene Coastal Loess Deposits of the Central West Coast of North America: Terrestrial Facies Indicators for Marine Low-Stand Intervals", *Aeolian Research*, Vol. 12, pp. 47-64. <https://doi.org/10.1016/j.aeolia.2013.11.001>
30. Popescu, R. and Chakraborty, P. (2006). "Liquefaction Mechanism for Heterogeneous Soils", *In: Proceedings Sea to Sky Geotechnique—59th Canadian Geotechnical Conference and Seventh Joint CGS/IAH-CNC Groundwater Specialty Conference*, pp. 1-4.
31. Polito, C.P. and Martin II, J.R. (2001). "Effects of Nonplastic Fines on the Liquefaction Resistance of Sands", *Journal of Geotechnical and Geoenvironmental Engineering*, Vol. 127, No. 5, pp. 08-415. [https://doi.org/10.1061/\(asce\)1090-0241\(2001\)127:5\(408\)](https://doi.org/10.1061/(asce)1090-0241(2001)127:5(408))
32. Presti, D.C.F., Lai, C.G. and Kaynia, A.M. (2016). "Determination of Small-Strain Stiffness of Soils and Soft Rocks Using Bender Element Tests", *Soil Dynamics and Earthquake Engineering*, Vol. 88, pp. 346-359.
33. Qian, X., Gray, D.H. and Woods, R.D. (1991). "Resonant Column Tests on Partially Saturated Sands", *Geotechnical Testing Journal*, Vol. 14, No. 3, pp. 266-275. <https://doi.org/10.1520/gtj10571j>
34. Raghunandan, M., Juneja, A. and Hsiung, B. (2012). "Preparation of Reconstituted Sand Samples in the Laboratory", *International Journal of Geotechnical Engineering*, Vol. 6, No. 1, pp. 125-131. <https://doi.org/10.3328/ijge.2012.06.01.125-131>
35. Saha, D. and Sahu, S. (2016). "A Decade of Investigations on Groundwater Arsenic Contamination in Middle Ganga Plain, India", *Environmental Geochemistry and Health*, Vol. 38, pp. 315-337. <https://doi.org/10.1007/s10653-015-9730-z>
36. Santamarina, J.C., Klein, A. and Fam, M.A. (2001). "Soils and Waves: Particulate Materials Behaviour, Characterization and Process Monitoring", *Journal of Soils and Sediments*, Vol. 1, No. 2, pp. 130-130. <https://doi.org/10.1007/bf02987719>
37. Sitharam, T.G., Govindaraju, L. and Srinivasa, M.B.R. (2004). "Evaluation of Liquefaction Potential and Dynamic Properties of Silty Sand Using Cyclic Triaxial Testing", *Geotechnical Testing Journal*, Vol. 27, No. 5, pp. 423-429. <https://doi.org/10.1520/gtj11894>
38. Tsukamoto, Y., Kawabe, S., Matsumoto, J. and Hagiwara, S. (2014). "Cyclic Resistance of Two Unsaturated Silty Sands Against Soil Liquefaction", *Soils and Foundations*, Vol. 54, No. 6, pp. 1094-1103. <https://doi.org/10.1016/j.sandf.2014.11.005>
39. Viana da Fonseca, A., Carvalho, J., Ferreira, C., Santos, J.A. and Almeida, F. (2009). "A Reappraisal of the Bender Element Testing Technique", *Geotechnical Testing Journal*, Vol. 32, No. 2, pp. 91-107.
40. Viggiani, G. and Atkinson, J.H. (1995). "Interpretation of Bender Element Tests", *Geotechnique*, Vol. 45, No. 1, pp. 149-154. <https://doi.org/10.1680/geot.1995.45.1.149>
41. Wijewickreme, D. and Sanin, M.V. (2006). "New Sample Holder for the Preparation of Undisturbed Fine-Grained Soil Specimens for Laboratory Element Testing", *Geotechnical Testing Journal*, Vol. 29, No. 3, pp. 242-249. <https://doi.org/10.1520/gtj12699>
42. Zamani, M. and Badv, K. (2019). "Assessment of the Geotechnical Behavior of Collapsible Soils: A Case Study of the Mohammad-Abad Railway Station Soil in Semnan", *Geotechnical and Geological Engineering*, Vol. 37, No. 4, pp. 2847-2860. <https://doi.org/10.1007/s10706-018-00800-1>
43. Thevanayagam, S., Fiorillo, M. and Liang, J. (2000). "Effect of Non-Plastic Fines on Undrained Cyclic Strength of Silty Sands", *In Soil Dynamics and Liquefaction*, pp. 77-91. [https://doi.org/10.1061/40520\(295\)6](https://doi.org/10.1061/40520(295)6)